Icarus 231 (2014) 365–376

Contents lists available at ScienceDirect

Icarus

journal homepage: www.elsevier.com/locate/icarus

HiRISE observations of Recurring Slope Lineae (RSL) during southern summer on Mars

Lujendra Ojha [a,1,*], Alfred McEwen [b], Colin Dundas [c], Shane Byrne [b], Sarah Mattson [b], James Wray [a], Marion Masse [d], Ethan Schaefer [b]

[a] University of Arizona, Lunar and Planetary Laboratory, 1541 E. University Blvd., Tucson, AZ 85721, United States
[b] Georgia Institute of Technology, School of Earth and Atmospheric Sciences, 311 Ferst Drive, Atlanta, GA 30332-0340, United States
[c] United States Geological Survey, Astrogeology Science Center, 2255 N. Gemini Dr., Flagstaff, AZ 86001, United States
[d] Institute of Geological Sciences, Polish Academy of Sciences, Research Center in Wrocław, ul. Podwale 75, 50-449 Wrocław, Poland

ARTICLE INFO

Article history:
Received 16 June 2013
Revised 7 November 2013
Accepted 23 December 2013
Available online 3 January 2014

Keyword:
Mars, surface
Geological processes
Ices

ABSTRACT

Recurring Slope Lineae (RSL) are active features on Mars that might require flowing water. Most examples observed through 2011 formed on steep, equator-facing slopes in the southern mid-latitudes. They form and grow during warm seasons and fade and often completely disappear during colder seasons, but recur over multiple Mars years. They are recognizable by their incremental growth, relatively low albedo and downhill orientation. We examined all images acquired by HiRISE during L_s 250–10° (slightly longer than southern summer, L_s 270–360°) of Mars years 30–31 (03/2011–10/2011), and supplemented our results with data from previous studies to better understand the geologic context and characteristics of RSL. We also confirmed candidate and likely sites from previous studies and discovered new RSL sites. We report 13 confirmed RSL sites, including the 7 in McEwen et al. (McEwen et al. [2011]. Science 333(6043), 740–743]. The observed seasonality, latitudinal and slope orientation preferences, and THEMIS brightness temperatures indicate that RSL require warm temperatures to form. We conclude that RSL are a unique phenomenon on Mars, clearly distinct from other slope processes that occur at high latitudes associated with seasonal CO_2 frost, and episodic mass wasting on equatorial slopes. However, only 41% (82 out of 200) of the sites that present apparently suitable conditions for RSL formation (steep, equator-facing rocky slopes with bedrock exposure) in the southern mid-latitudes (28–60°S) contain any candidate RSL, with confirmed RSL present only in 7% (13 sites) of those locations. Significant variability in abundance, size and exact location of RSL is also observed at most sites, indicating additional controls such as availability of water or salts that might be playing a crucial role.

1. Introduction

Liquid water is a key requirement for life on Earth. The presence of liquid water on Mars' present-day surface would therefore have significant implications for possible astrobiology, and could also prove pivotal for future human exploration. There are numerous geomorphological lines of evidence for the past existence of flowing water on Mars (e.g. Baker, 1982; McCauley et al., 1972; Carr, 1995 and references within) but whether liquid water can exist on current day Mars has been controversial (e.g., Zent et al., 1990; Hecht, 2002). Pure water would rapidly evaporate and/or freeze on the present-day surface of Mars at most times and places; however, brines are far less volatile compared to pure water due to their lower freezing points and evaporation rates (e.g. Brass, 1980; Chevrier and Altheide, 2008).

Recurring Slope Lineae (RSL) are relatively low-albedo features that extend incrementally downslope on steep equator-facing rocky slopes on Mars, and recur in multiple Mars years (MY) (McEwen et al., 2011). (Mars years are abbreviated MY, and MY 1 started at L_s 0° on 11 April 1955 (Clancy et al., 2000) L_s is the areocentric longitude of the Sun, a measure of season on Mars. Southern summer begins at L_s 270°). They range in width from about 5 m down to the limits of HiRISE detection (~0.25 m/pixel), and up to a few hundred meters in length (Fig. 1). They were first observed by the High Resolution Imaging Science Experiment (HiRISE) (McEwen et al., 2007) on the Mars Reconnaissance Orbiter (MRO) (Zurek and Smrekar, 2007). The following description summarizes observations made in the initial description of RSL by McEwen et al. (2011). They are often associated with small channels or gullies, and occasionally with the larger gully landforms

* Corresponding author.
E-mail addresses: luju@gatech.edu (L. Ojha), mcewen@pirlmail.lpl.arizona.edu (A. McEwen), cdundas@usgs.gov (C. Dundas), shane@lpl.arizona.edu (S. Byrne), smattson@pirlmail.lpl.arizona.edu (S. Mattson), jwray@eas.gatech.edu (J. Wray), marion.masse@twarda.pan.pl (M. Masse), Schaefer@lpl.arizona.edu (E. Schaefer).
[1] Present address: Georgia Institute of Technology, United States.

0019-1035/$ - see front matter © 2013 Elsevier Inc. All rights reserved.
http://dx.doi.org/10.1016/j.icarus.2013.12.021

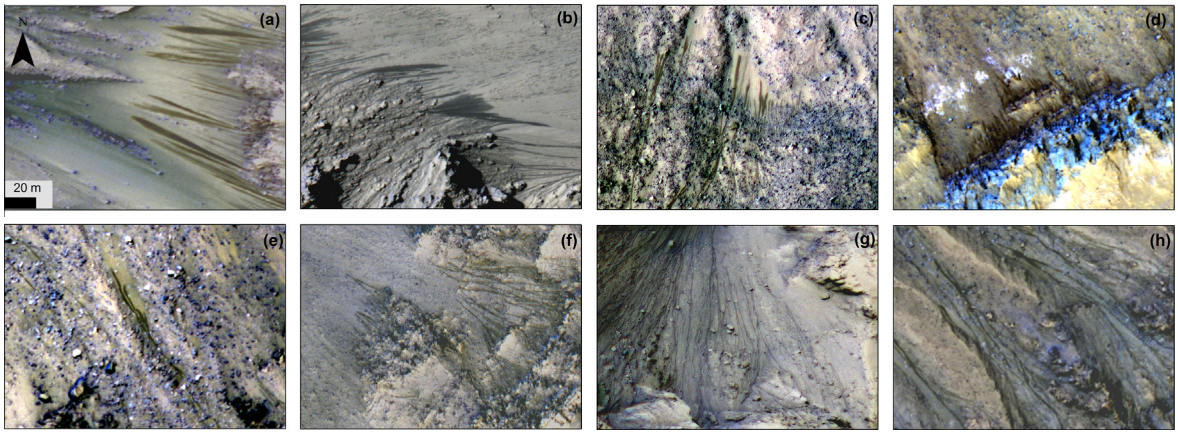

Fig. 1. Variety of RSL observed in HiRISE images. From top left to bottom right: (a) ESP_022689_1380, (b) PSP_005787_1475, (c) ESP_013835_1330, (d) PSP_006261_1410, (e) ESP_014288_1315, (f) PSP_005524_1470, (g) PSP_005646_1360, (h) ESP_022973_1335. The downhill direction is along the elongated path of RSL. North is up. Images have been manually stretched.

described by Malin and Edgett (2000). At some locations, RSL are observed in small numbers (tens of lineae), but in other locations hundreds or thousands of them may occur (Fig. 1). Lineae can form anastomosing patterns, branching and rejoining, although this could be from flows that are separate in time but spatially overlap. In the southern mid-latitudes, RSL form and incrementally lengthen during the late southern spring through summer, most commonly on equator-facing (and east- and west-facing) slopes with good bedrock exposures or rocky slopes that probably indicate shallow bedrock. They occur on geomorphically fresh slopes, devoid of surface features that require years to form, (e.g., significant mantling deposits, eolian bedforms or polygons). These slopes are near the expected "angle of repose" or critical inclination angle on which a sufficient thickness of dry cohesionless particles can flow (Pouliquen, 1999), so active mass wasting is to be expected. At the times and places where RSL are active, the surface temperatures derived from the Thermal Emission Imaging System (THEMIS; Christensen et al., 2004) Brightness Temperature Record (BTR) and Projected Brightness Temperature (PBT) images can be above 273 K at some places. Higher peak temperatures (~270–310 K) were suggested by Stillman et al. (2013) from analysis of ~2 PM observations (at ~3 km spatial resolution) by the Thermal Emission Spectrometer (TES: Christensen et al., 2001). RSL were initially found concentrated in the southern middle latitudes, and found to be active during southern summer, but were recently found in equatorial sites in Valles Marineris where they are active in different seasons (McEwen et al., 2014).

McEwen et al. (2011) briefly considered several formation mechanisms for RSL, including dry mass wasting, wet debris flows, and surface or sub-surface flow of saline water. RSL like morphology could be a result of dry mass wasting triggered by seasonally high winds or dust devils, however, the rarity of RSL in the northern hemisphere is left unexplained. Dry mass wasting also does not explain their incremental growth, nor their slope orientation preference in the southern middle latitudes. CO_2 sublimation drives many other dynamic phenomena on Mars (e.g., Hansen et al., 2011; Diniega et al., 2011; Dundas and Bryne, 2010), including gully erosion and modification (Dundas et al., 2012a,b), but RSL occur at times and places that are among the warmest on Mars, where CO_2 frost cannot form or persist. The latitudinal and seasonal characteristics of RSL and their association with temperatures greater than 240 K suggested a formation mechanism involving briny water (McEwen et al., 2011). Although pure water is not stable on the surface of Mars, salts can lower the freezing point by up to 70 K and lower the evaporation rates by factors of 10 or more, making salty water more stable than pure water (Brass, 1980; Hecht, 2002; Chevrier and Altheide, 2008; many others).

Here we document the morphological, geological and thermal characteristics of RSL in the southern mid-latitudes to provide constraints on their origin. Much variability is observed with the general morphology of RSL at different sites, which we describe in detail in Section 3. Due to observed seasonality, lack of observations and/or ambiguity involved in distinguishing RSL from other features we have divided RSL into different kinds, which we describe in detail in Section 4. The limits of RSL distribution in latitude and elevation are also addressed in this section. RSL form on very specific slope types, which we describe in Section 5. The seasonality, surface temperature and inter-annual variability of RSL are addressed in Section 6.

Although we provide details of different kinds of RSL in Section 4, below we provide short definition of each to assist in the methodology section:

(a) *Confirmed:* RSL that are observed to grow incrementally and recur in multiple MY.
(b) *Partially confirmed:* RSL that are either observed to grow incrementally or recur in multiple years, but not both.
(c) *Candidate:* lineaes observed on slopes but without verification for incremental growth or recurrence (see Section 4 for more details).

2. Data sets and methods

2.1. HiRISE

Since the initial discovery of RSL, specific sites were frequently monitored with HiRISE in the latter half of MY 30 and in MY 31 (which is ongoing at the time of writing), to better understand their geographical distribution and environmental clues to their formation mechanism. We especially wanted to know how common RSL are on Mars in the environment where they are normally observed (steep, rocky, warm slopes). HiRISE acquired 1984 observations over all latitudes (89°S to 85°N) between L_s 250–10° of MY 30 and MY 31 at resolution up to ~25 cm/pixel (Fig. 2). We examined browse versions, which are lower in resolution than normal HiRISE images, (McEwen et al., 2010) of all images acquired between L_s 250–360° for MY 30 and L_s 0–10° for MY 31 in search of steep slopes (probably > 20°). Steep, high slopes (at all slope orientations and all latitudes) identified in this way were then examined at full resolution to look for RSL. We tabulated the nature of steep

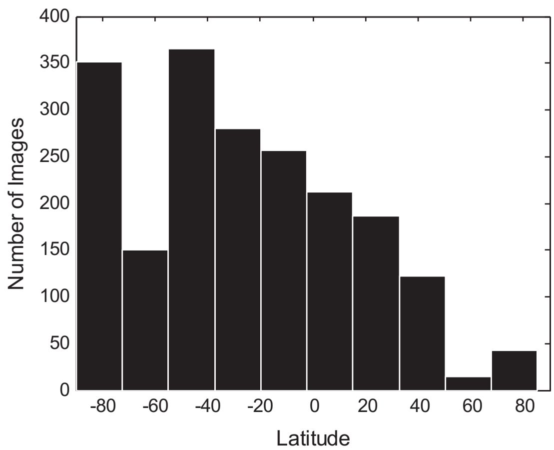

Fig. 2. Number of HiRISE observations vs. latitude from L_s 250–360° of MY 30 and L_s 0–10° of MY.

slopes (presence of bedrock outcrops and/or loose boulders, abundance of channels and gullies, and slope orientation) and the presence/absence of candidate RSL to understand the importance of the nature of slopes for RSL formation. When potential RSL were observed, we examined any other overlapping images, if available, to study their time variability. We supplemented our results with data from previous studies to classify observed lineae into different classes (Section 4). We also tabulated the exact location of confirmed RSL (RSL that exhibit incremental growth and recur in multiple years) and tabulated the thermal inertia, albedo, and dust index data for those locations. HiRISE Digital Terrain Models (DTMs) along with their associated orthorectified images for eight RSL sites were used to derive slope values to observe any difference between the starting and ending slopes using BAE SOCET SET and ArcGIS. (Table S1 lists HiRISE image IDs, with their locations, for confirmed, partially-confirmed and candidate RSL (see Section 4 for full description) sites observed in MY 30 and MY 31 in addition to sites from previous years).

2.2. THEMIS

THEMIS BTR and PBT images were used to extract surface temperatures of RSL slopes. Brightness temperature assumes isotropic emission, unit emissivity and zero atmospheric optical depth, so these are minimum values for actual kinetic temperatures of the surface. The atmosphere is generally colder than the surface, yielding lower apparent temperature, but we only derived surface temperature from images that were relatively dust free and transparent. The THEMIS images were found using the overlap tool in JMARS (Gorelick et al., 2003) and were then rendered on top of HiRISE images and average temperatures of RSL slopes were acquired. At places where we see RSL in multiple slope orientations we averaged the temperature values to derive a mean slope temperature for RSL. The PBT THEMIS images are well registered with HiRISE, but occasionally need some manual adjustment for a better fit. The BTR images are not projected, so image geo-referencing was conducted within JMARS and ArcGIS for a precise alignment with HiRISE images (Table S2 lists confirmed RSL and partially confirmed sites (whose recurrence has been verified) by their HiRISE image ID center latitude and center longitude, and THEMIS observation IDs that were used to derive surface temperature. Other surface properties like albedo and thermal inertia are also reported.). We also used thermal modeling (e.g., Hansen et al., 2012; Dundas and Byrne, 2010) at all confirmed RSL sites to estimate surface temperatures at times and places where we lacked THEMIS observations.

3. General morphology of RSL

RSL are distinct from their surroundings due to their lower albedo (up to 40% darker than the surroundings, at least in MY 28 after dust storms brightened the surface) (McEwen et al., 2011), narrow width (up to ~5 m, but commonly less) and orientation directly down the topographic gradient. Some lineae are at the limits of HiRISE detection due to a combination of small size and low contrast, especially from dustiness of the atmosphere. They have lengths up to hundreds of meters and thousands of them may be present in clusters on slopes facing the equator, west and/or east. Occasionally they are seen on pole-facing slopes, especially at relatively low latitudes (32–36°S) like Horowitz crater or Hale crater. RSL usually originate from bedrock outcrops or rocky areas and are observed to divert around obstacles, rather than overtopping them (Figs. 1 and 3, and others). They are often associated with small gullies, and occasionally with larger gully landforms (Fig. 1). Lineae can form anastomosing patterns, branching and rejoining, although this could be from flows that are separate in time but spatially overlap. We have also observed relatively bright and smooth fans or aprons at all confirmed RSL sites in the southern mid-latitude, with lineae often extending to near the fan terminus (Figs. 1 and 3). The bright fans are either associated with individual lineae (if they are isolated) or a group of them (e.g. Palikir crater—Fig. 4). These fans encompass wider areas than the lineae and at HiRISE resolution seem to be composed of homogenous fine-grained material without any inclusion of resolvable boulders. The abundance and spatial relation of fans with RSL suggest formation mechanisms that are interdependent, but it is not clear whether RSL deposit the fans, or the fans provide conditions that allow RSL to form or be seen.

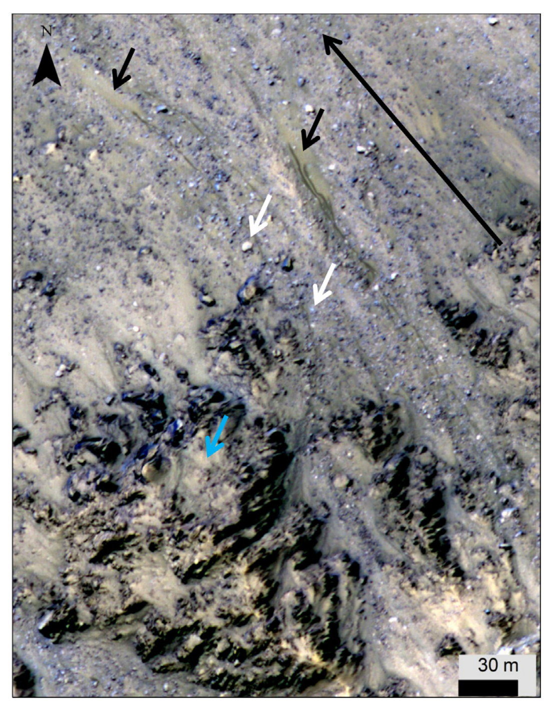

Fig. 3. Morphology of RSL slope in ESP_014288_1315. Blue arrow pointing to bedrock exposure. White arrows pointing to abundance of loose boulders on RSL slopes. Black arrows pointing to RSL and fans around it. Long black arrow on the upper right pointing towards the downslope direction. Note the absence of polygons and eolian bedfroms on this slope. (For interpretation of the references to color in this figure legend, the reader is referred to the web version of this article.)

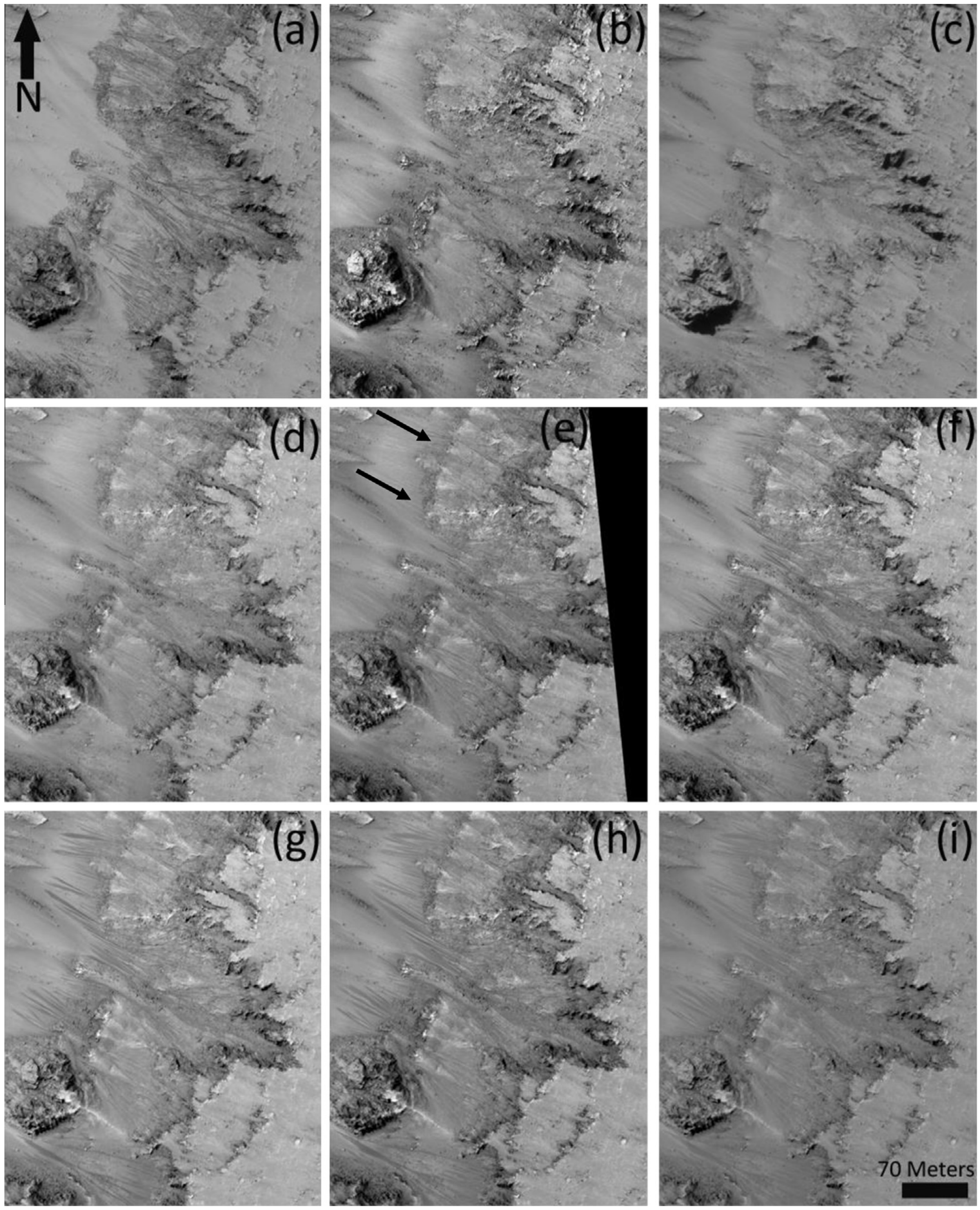

Fig. 4. RSL at Palikir crater. (a) PSP_005943_1380, MY: 28, L_s: 341° show RSL on NW facing slope. The downhill direction in this and all other image is to upper left. (b) ESP_011428_1380, MY: 29, L_s: 184°, RSL not observed in this image. (c) ESP_016808_1380, MY: 30, L_s: 57°, RSL not observed in this image. (d) ESP_021555_1380, MY: 30, L_s: 247°, RSL have not started to form yet. (e) ESP_021911_1380, MY 30, L_s: 265°, arrow points to area where RSL have started to form. (f) ESP_022267_1380, MY: 30, L_s: 282°, compared to ESP_021911_1380 RSL have grown. (g) ESP_022689_1380, MY: 30, L_s: 302°, RSL growth observed compared to previous observations. (h) ESP_022834_1380, MY: 30, L_s: 309°, no RSL activity observed anymore. A little fading is also observed. (i) ESP_023045_1380, MY: 30, L_s: 318°, RSL have faded.

4. Types of RSL and geographical distribution

RSL are assigned to three categories: Confirmed, Partially Confirmed and Candidate (Table S3). All of them have the general morphology of RSL described above, and multiple (>10) lineae over a slope. There is ambiguity involved in distinguishing RSL from other types of slope lineations (dust avalanches, grain flows, boulder tracks) when we lack repeat observations to observe incremental growth, fading, and/or seasonal recurrence.

4.1. Confirmed RSL

Confirmed RSL are observed to grow incrementally during a warm season, fade or completely disappear in colder seasons, and to recur during multiple warm seasons (Fig. 4). Prior to this work, only 7 sites were categorized as having confirmed RSL between 30°S and 60°S (McEwen et al., 2011). We have now identified 13 confirmed RSL sites in the southern mid-latitudes (Fig. 5). Two candidate and four partially confirmed sites from McEwen et al. (2011) are now confirmed in addition to one new site that was not reported in McEwen et al. (2011). Additionally, 15 new confirmed or partially confirmed RSL sites have been discovered in the equatorial region. Those sites are described in McEwen et al. (2014).

4.2. Partially confirmed RSL

Partially confirmed RSL have the morphology and geological setting of confirmed RSL. We either observe incremental growth

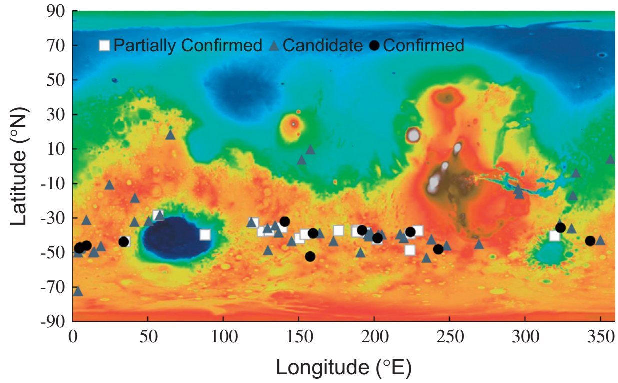

Fig. 5. Geographical distribution of confirmed, partially confirmed and candidate RSL sites.

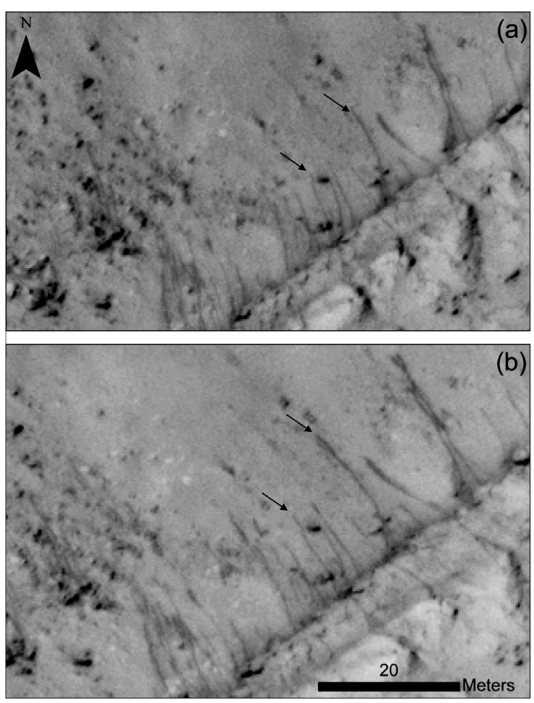

Fig. 6. Partially confirmed RSL in a fresh crater at 42°S, 151°E. Arrows point to lineae in (a) (ESP_022174_1310, MY: 30, L_s: 277°) observed to have grown in (b) (ESP_023097_1310, MY: 30, L_s: 320°). These lineae are considered partially confirmed rather than confirmed because, although it has the morphology and geological setting of confirmed RSL and incremental growth is observed, we have not been able to confirm their recurrence. Recurrence has been confirmed for few other partially confirmed RSL sites, but incremental growth has not been observed due to lack of repeat coverage.

and/or fading, or recurrence, but not both, generally due to lack of suitable repeat observations. For full confirmation, we need to observe all of the above criteria, so we classify them as being partially confirmed. Fig. 6 shows an example, where these features have the geological and morphological characteristics of RSL. Incremental growth is observed for some lineae, but recurrence is not yet verified. There are 20 partially confirmed RSL sites, 8 based on recurrence and 12 based on incremental growth and/or fading, all in the southern mid-latitudes (Fig. 5). McEwen et al. (2011) reported 10 unique likely RSL sites (partially confirmed RSL sites were termed likely in that work) in the southern mid-latitudes out of which 4 have been confirmed now. Most of the remaining partially confirmed or candidate RSL sites from McEwen et al. (2011) lack the multiple observations necessary to be classified as confirmed RSL.

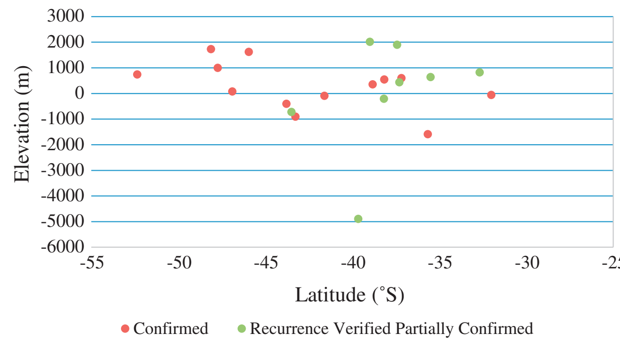

Fig. 7. Latitude vs. elevation for confirmed and partially confirmed RSL sites whose recurrence has been confirmed.

4.3. Candidate RSL

Candidate RSL have the morphology and setting (at least steep slopes) of RSL but neither fading/incremental growth nor recurrence has been observed. The resolved lineae are sometimes fewer in number (<10) on a slope, or may be near the limit of detection by HiRISE. The lack of repeat observations, coupled with their small size makes it hard to distinguish candidate RSL from lineae produced by episodic mass wasting or topographic shading. The geographical distribution of candidate RSL is much more widespread than confirmed RSL due to this uncertainty. We have found 49 candidate RSL sites between 72°S and 19°N (Fig. 5).

4.4. Global distribution

The range of elevation for confirmed and partially confirmed RSL sites based on their recurrence from the southern mid-latitudes is −5 to +2 km (mean ~ 172 m) (Fig. 7). There are only three sites occurring below −1 km, but there are limited low areas in the southern highlands and those regions (mainly Hellas and Argyre basins) are often obscured by atmospheric dust and haze. There are also many RSL at low elevations in Valles Marineris (McEwen et al., 2014).

5. Geological setting and surface properties

5.1. Slope orientation

RSL in the southern mid-latitudes usually form on equator- and west- or east-facing slopes. Fig. 8 shows different slope orientations imaged in HiRISE observations of RSL sites (excluding repeat images of the same site) and the fraction of slopes where RSL are actually observed. Although RSL usually form on equator-facing slopes, there are some sites where we observe RSL on pole-facing slopes, such as Horowitz crater at 32°S. Some, but not all, of the pole-facing RSL lie at lower latitudes, where the slope receives significant insolation near summer solstice. Pole-facing slopes receive less radiance from the Sun and are colder, which might explain why RSL are less abundant there (Hecht, 2002). Also, RSL on east-facing slopes are observed less often than west-facing slopes, which may be due to an observational bias as MRO acquires images at approximately 3:00 PM local time (Zurek and Smrekar, 2007), when east-facing slopes are largely shaded.

5.2. Steepness of the slopes

RSL slopes have concave topographic profiles. The average starting slope derived from 8 HiRISE DTMs of confirmed RSL sites is 33°, and the ending slopes have a mean of 27°. We have not observed

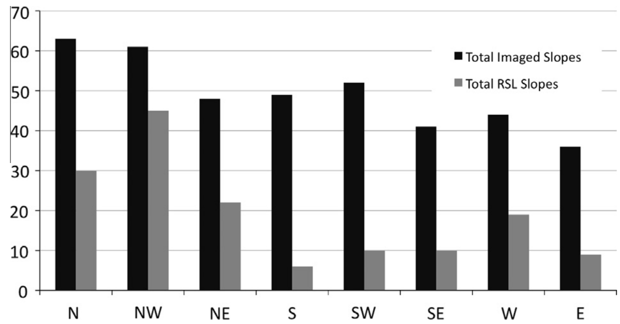

Fig. 8. Total imaged slopes corresponds to number of times a particular slope orientation was imaged through HiRISE in Table S1, and total RSL slopes corresponds to the fraction of those images where RSL were observed.

any site where RSL have flowed down to the bottom of a slope in the southern mid-latitudes. Because RSL are terminating on shallower slopes—but steep enough for either liquid or dry cohesionless flows to continue in many cases (Pouliquen, 1999)—their length is likely controlled by a limited volume of mobile material.

5.3. Surface properties

RSL occur on steep slopes that appear geologically very recent, and are often found in "fresh" (well-preserved) impact craters. The slopes look geomorphically active since they have bedrock exposure, loose boulders, minimal dust cover (based on visual inspection), may be covered by numerous small channels, and are not covered by smaller impact craters, eolian bedforms, or periglacial patterns that suggest a relatively young landscape. (Fig. 9). The pole-facing slopes of these impact craters are often dominated by large gully landforms (ravines) like those described by Malin and Edgett (2000), but RSL are rarely found on the large-gullied slopes. In some cases, they instead occur on slopes facing the larger ravines. Confirmed RSL sites found at mid-latitudes have low dust cover (1350–1400 cm^{-1} wavelength emissivity ranging from 0.96 to 0.98, mean 0.97 (Maximum dust cover corresponds to values close to 0.89 and minimum dust cover index are closer to 0.99.); Ruff and Christensen, 2002), moderate thermal inertia of 193–692 $J\,m^{-2}\,s^{-1/2}\,K^{-1}$ (with a mean of 240 $J\,m^{-2}\,s^{-1/2}\,K^{-1}$), and low albedo 0.1–0.17 (with a mean of 0.14). The mean thermal inertia and albedo imply surfaces composed of coarse-grained sediments, with bedrock exposure and perhaps some duricrust (Presley and Christensen, 1997; Mellon et al., 2000; Putzig et al., 2005). As RSL typically begin from rocky areas or bedrock, the local thermal inertia at the source is certainly higher. Dust cover index and albedo are also derived from lower-resolution data, while RSL are very local phenomena.

The 13 confirmed RSL locations have elevations, albedos and nighttime thermal inertias summarized in Table S2. We can ask whether these properties at RSL sites are different than the typical values found within this latitude band (32–52°S). To do this we use the non-parametric Mann–Whitney U-Test, which is more appropriate in this situation than a standard *T*-test as the distribution of these quantities is far from Gaussian. The null hypothesis is that the population of RSL sites is the same as the general mid-latitude population when considering things like elevation, albedo and thermal inertia. The test evaluates the probability that the null hypothesis is true and a result of 5% or less would indicate that the RSL sites are distinct from the rest of the mid-latitudes in a statistically significant way.

Our results indicate that the albedos and elevations of the population of RSL sites are different from the rest of the mid-latitudes (test results of 0.1% and 1% respectively), but that the thermal

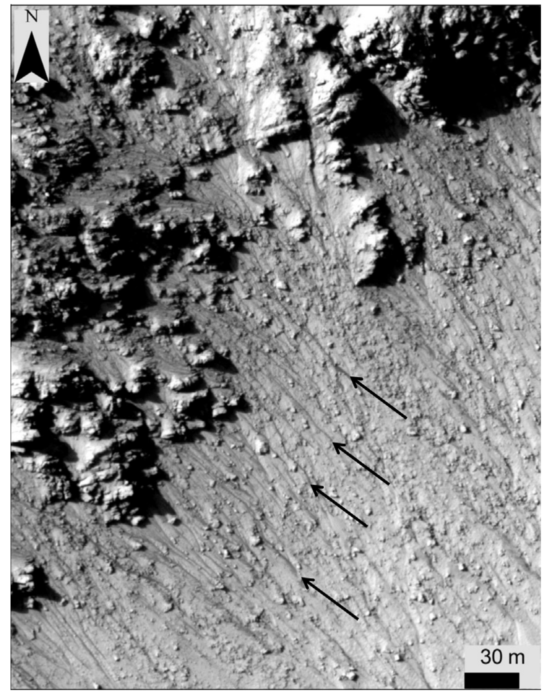

Fig. 9. Slope in Horowitz crater (PSP_005787_1475) with numerous small channels (a few indicated by black arrows). RSL follow these channels.

inertia of this population does not differ appreciably (test result of 22%). What does 'different' mean in this context? The answer is not straightforward as the test is sensitive to both distribution-shape and median-value differences between the two populations being compared. The most common assumption when interpreting the results of this test is that the shape of the two distributions is close enough so that this is really a test of whether the median values of the populations differ significantly. With this assumption, we can say the RSL sites are darker and lower in elevation than average mid-latitude terrain in a statistically significant way. There is some ambiguity in the elevation result however as, when the Hellas and Argyre basins are excluded, there is a weak correlation between albedo and elevation.

6. Seasonality, surface temperature and inter-annual variability

6.1. Seasonality

Confirmed RSL in the southern mid-latitudes are observed to form and grow during southern summer. Fig. 10 shows seasonality of confirmed RSL from three different MY. In MY 28 RSL are observed to form as early as L_s 250°, and incremental growth occurring as late as L_s 11–20°. In MY 29 and 30, incremental growth for RSL was short-lived. We did not observe incremental growth occurring past L_s 340°. RSL fade during late summer and often completely disappear during the colder seasons (L_s 20–250°). At some sites, lineae are observed to fade while adjacent RSL are still active (incremental growth and darkening observed) during southern summer. RSL sites from the equatorial region show a different kind of seasonality as a function of slope orientation, but have not yet been characterized through a complete Mars year (McEwen et al., 2014). Incremental growth for partially confirmed RSL also occurs during southern summer. The seasonal behavior of candidate RSL is unconstrained; where repeat imaging is available, we either do not observe any activity or the time separation between the images is large.

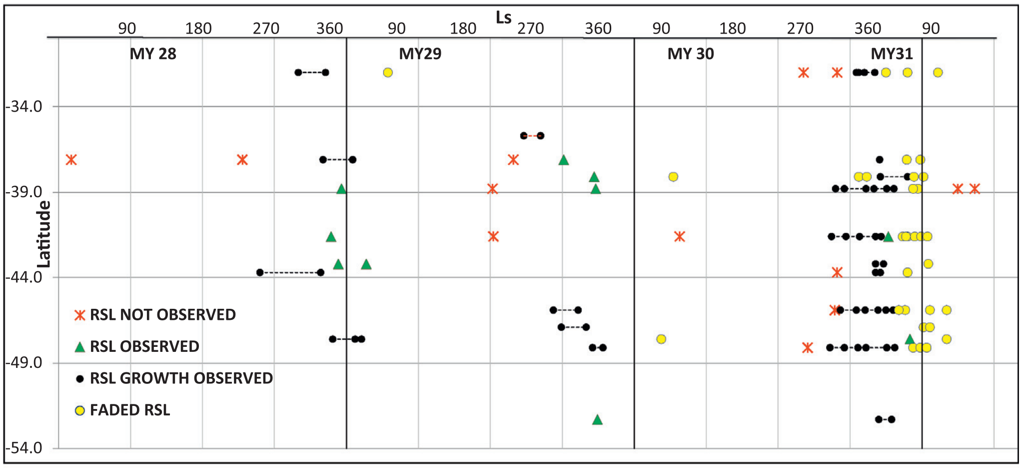

Fig. 10. Seasonality of confirmed RSL. Dotted lines between "RSL Growth Observed" points indicate the range of L_s during which the RSL were observed to be incrementally growing. RSL growth could have ended anytime between the last two "RSL growth observed" images, so there only two clear cases in which growth continued beyond L_s 360. Red dashed line between two points at 35S is for Hale Crater, for which we only have two images at the L_s range of our survey. However, recurrence has been confirmed for this site from images of MY 31 southern summer.

6.2. Surface temperature

THEMIS BTR and PBT images were used to estimate surface temperatures of RSL locations (Fig. 11) at times when THEMIS observations were available. The temperatures listed in Tables S2 and S4 are averaged over all RSL slopes at each site due to the coarse resolution (~100 m/pixel) of THEMIS BTR and PBT images. The "RSL Slope orientation" column in Table S2 lists different slopes averaged to derive a mean temperature of the RSL location. During the southern summer (L_s 250–360°) when most RSL form, incrementally grow, and start fading, the observed surface temperature ranges between 240 K and 290 K in equator-, west- and east-facing slopes of RSL sites (Table S2). Most of the THEMIS observations were acquired between 2:00 and 4:00 PM, so we observe the peak temperature on NW-facing slopes, and the peak temperature on NE- and N-facing slopes occurs earlier in the day.

During the L_s range when we observe RSL growth, the temperature ranges between 252 K and 290 K (Table S4). However, some of the temperature values correspond to MY 26 and 27, predating the arrival of HiRISE/MRO to Mars. There are also seven sites in Table S4 that do not have THEMIS images from any year for the L_s range of RSL growth.

Given the late time of day of THEMIS observations and lack of data a thermal model is required to investigate the peak temperatures reached on most of these slopes. This model is based on (and described in more detail within) that used by Hansen et al. (2012). In short, the model solves conductive heat exchange with the subsurface driven by the surface radiative balance in a semi-implicit way. Surface insolation is slope dependent and these sloping surfaces also receive reflected and emitted radiation from the surround flat terrain. We separately simulate surface temperatures for this surrounding flat terrain using the regional values for thermal inertia and albedo at these locations derived from TES (e.g. Putzig and Mellon, 2007; Christensen et al., 2001) and shown in Table S2. We use the regional albedo for the sloping surfaces too and for simplicity consider only 30° north-equator-facing slopes. The choice of thermal inertia is somewhat problematic as these slopes are rockier than the surrounding region and so would be expected to have higher thermal inertia. As one end member we use the regional value for the slope too. We also compared the available summer night-time temperatures on these slopes from THEMIS and found the model best reproduced them with a thermal

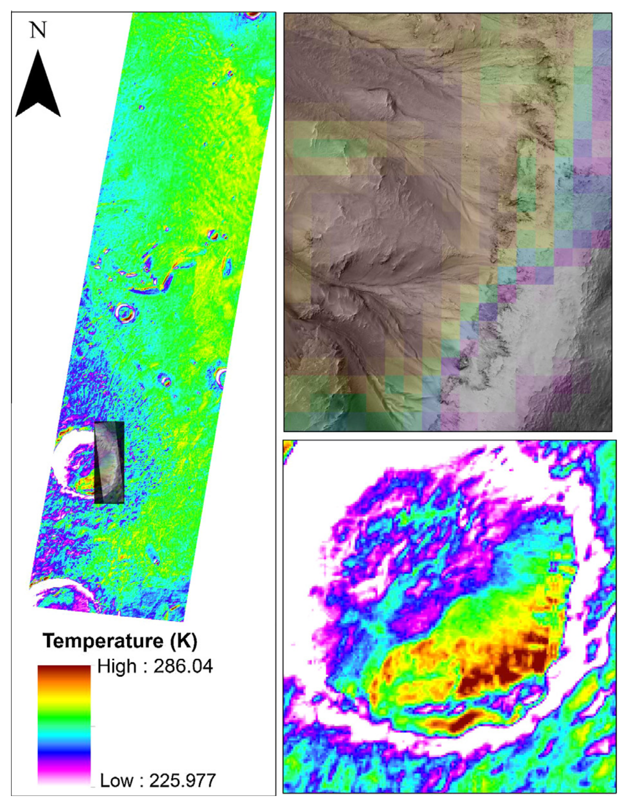

Fig. 11. THEMIS PBT image I34263004 (L_s: 332°, Local Solar Time: 14.5) with HiRISE observation PSP_005943_1380 (Lat: −41.6°, Lon: 202.3°). THEMIS PBT image was stretched manually to observe the range of temperature surrounding RSL region (small arrows pointing to RSL slope). The RSL slope is observed to be much warmer than the surrounding. White area represents area that has much lower temperature than 225 K. White areas facing SE are under shadows.

inertia of 425 $J\,m^{-2}\,s^{-1/2}\,K^{-1}$. Model results for all 13 confirmed RSL sites are shown for these two values of thermal inertia in Fig. 12.

Daily peak temperatures at the surface and at a depth of 10 cm are shown in Fig. 12a and b. The timing of perihelion (L_s 252) results in a broad plateau of peak temperatures throughout the southern summer with all sites exhibiting similar behavior. Peak surface temperatures exceed 273 K most days of the year. Fig. 12c and d shows how many hours per day 273 K is exceeded at the surface, ranging from zero during the winter to 8 h/day for some sites near summer solstice. At depths of 10 cm the peak temperature does not exceed 273 K at any of these sites at any season. These model results indicate that if pure liquid water is involved in RSL formation that it must be at very shallow depths.

We also ran the same model using regional thermal inertia values reported in Table S2 without much difference in the result (Fig. 12b). During the L_s range of 250–360°, the confirmed RSL sites can have as much as 8 h per day of peak temperature above 273 K (Fig. 12c and d). We also occasionally observe RSL on pole-facing slopes, where the measured surface temperature lies in the range of 230–260 K (Table S2). However, THEMIS is missing the peak temperature in these slopes, so the 230–260 K is a lower estimate. In Fig. 13, the peak temperatures observed in all THEMIS images are plotted with no constraint on what season the images were acquired in. The annual peak temperatures are considerably lower in the northern mid-latitudes, which may explain why RSL are not observed there. The region from 10°N to 60°S is characterized by peak temperatures between ~280–310 K (Fig. 13).

6.3. Inter-annual variability

RSL exhibit substantial inter-annual variability. In a case study of Horowitz crater, RSL were observed in both MY 28 and MY 30,

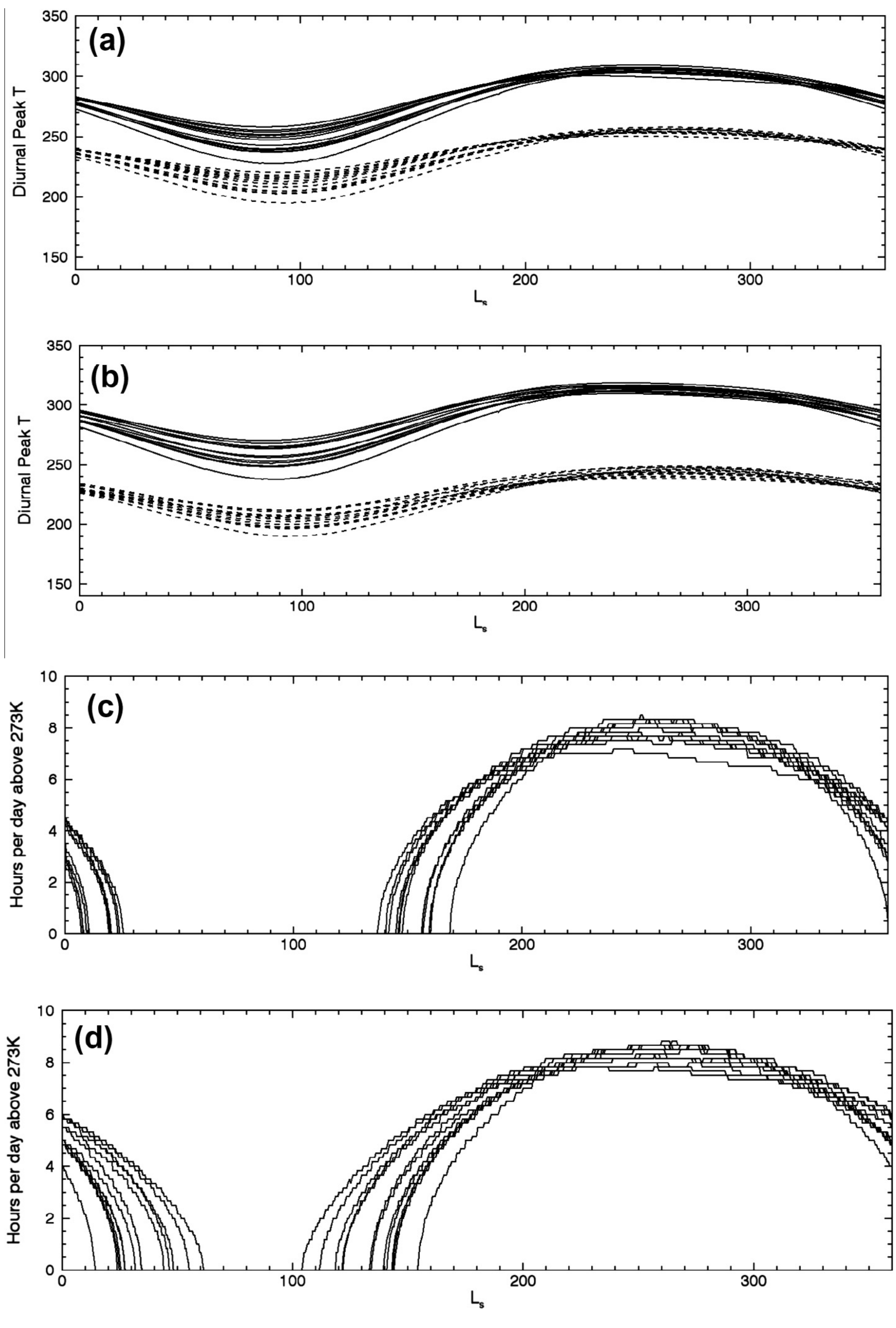

Fig. 12. (a) Diurnal peak temperature as a function of L_s for all confirmed RSL sites from southern mid-latitude for a 30° equator facing slope with thermal inertia of 425 J m^{-2} s$^{-1/2}$ K^{-1}. Solid line represents surface temperature, and dashed lines represent temperature at 10 cm depth. (b) Same as (a) using regional thermal inertia listed in Table S2. (c) Number of hours per day with peak temperature above 273 K as a function of L_s using parameters same as (a). (d) Same as (c) using regional thermal inertia listed in Table S2.

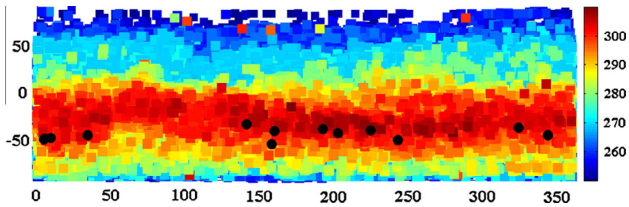

Fig. 13. Temperature map composed of all THEMIS images. Images with temperature between 250 K and 360 K were queried, and the latitude, longitude of each image was plotted with the peak temperature. The map shows higher temperature from latitude 10°N–60°S. Black round dots represent location of confirmed RSL.

but the activity and number of RSL in MY 30 was significantly less than in MY 28. In some other regions the duration of the activity was also shorter in MY 30–31 than in MY 28–29 (Fig. 14). Due to lack of observations or imperfect timing of observations, at some locations activity is observed in some Mars years but not in others. Temperatures from year to year on Mars are relatively similar apart from the effect of dust storms. A comprehensive study of inter-annual variability at various RSL locations is in progress. See McEwen et al. (2014) for more discussion of this issue.

7. Presence of RSL in favorable environments

In the southern mid-latitudes, RSL are found to be active during southern summer. HiRISE acquired ~2000 images of ~1700 sites during the MY 30–31 southern summer over all latitudes (90°S to 85°N) (Fig. 2). In the southern mid-latitudes (30°S to 60°S) HiRISE acquired images of ~500 unique sites. We observed ~200 sites with fresh equator-facing slopes with good bedrock exposure, the setting that seems necessary for RSL formation (McEwen et al., 2011). In some instances, the only visible difference between RSL bearing and non-RSL bearing slopes is the presence/absence of RSL. However, confirmed RSL were only found in 13 locations (7% of the sites) (Fig. 15). Additionally, we found partially confirmed RSL at 20 locations and candidate RSL in 49 locations. The true frequency of RSL may be even less, because many sites imaged in MY 30 were targeted specifically to look at known or suspected RSL and some of the sites of candidate or partially confirmed RSL were only imaged in MY 28 and 29 (when RSL were apparently more active). The rarity of RSL at southern mid-latitudes during southern summer in places with geological settings seemingly appropriate for RSL implies that other variables must have a substantial effect on where RSL can form and be apparent in HiRISE image.

Temperature differences between different sites could conceivably explain the location bias for RSL, but the entire southern mid-latitudes experiences high temperatures during southern summer, so we do not think this is the reason for the absence of RSL from geologically similar slopes. Other unknown factors, perhaps presence of salts or other compositional factors, must be responsible for this effect. However, compositional data have not been able to support this hypothesis, although the detection of sub-surface salt could be impeded by a thin layer of martian dust (Ojha et al., 2013). Availability of water may be the most obvious possibility.

8. Discussion

8.1. Limitations of survey methodology

It is not practical to search every HiRISE image at full resolution for RSL. From previous studies we know that RSL in the southern

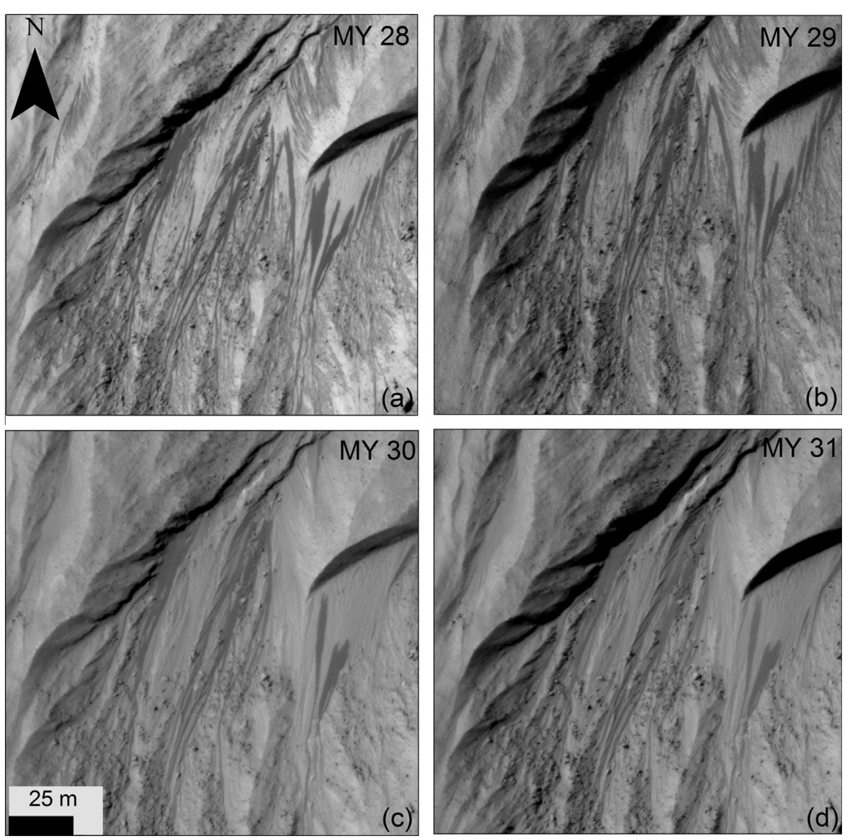

Fig. 14. Central hill of Lohse crater at 43°S, 343°E. (a) PSP_006162_1365, MY: 28, L_s: 341°, (b) PSP_007085_1365, MY: 29, L_s: 25°, (c) ESP_022908_1365, MY: 30, L_s: 312° and (d) ESP_024253_1365, MY: 31, L_s: 8°. The number of RSL in the MY 30/31 RSL season is significantly less than in the MY 28/29 season. No new RSL growth is seen in the later image of each pair, so this represents the maximum extent of RSL for each season.

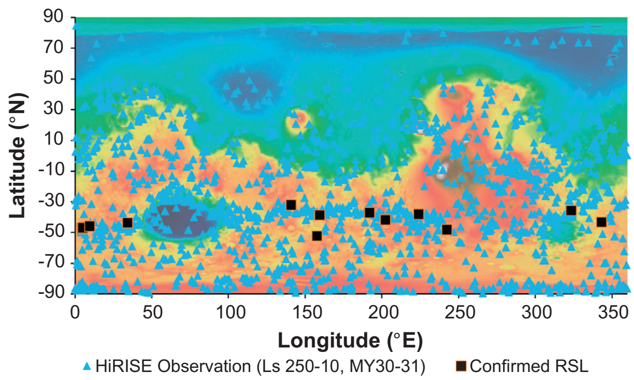

Fig. 15. (a) Distribution of HiRISE observations between L_s 250–10° of MY 30–31 (in blue). Distribution of confirmed RSL (in black). The background map is the topography of Mars. The concentration of images near latitude 40°S is due to targeting both RSL and gullies (see Fig. 2). (For interpretation of the references to color in this figure legend, the reader is referred to the web version of this article.)

mid-latitudes tend to form during southern summer (McEwen et al., 2011). Although negative results are not described in detail in this paper we did examine hundreds of locations from the equatorial and northern hemisphere regions during appropriate seasons for signs of RSL. The main data set corresponding to L_s 250–10° falls during northern winter, so we may have not observed RSL due to the lower temperature or other unfavorable seasonal factors. Data from previous years exist to address this deficiency, but we have not done so in this paper. We have found a few candidate RSL in the northern hemisphere; two locations are partially confirmed (McEwen et al., 2014), but show very minor incremental growth. We also examined images of hundreds of fresh craters from both hemispheres at all seasons to look for RSL. The high latitudes (>60°N and S) are well sampled (although less sampled than the mid-latitudes) by HiRISE, but the temperatures there are much lower, and there are few steep slopes due to ice-related processes (e.g., Kreslavsky and Head, 2003). An additional bias is that HiRISE images are deliberately targeted on sites expected to be interesting at high resolution, such as fresh steep slopes. However, to date almost all documented RSL are in such settings, and conclusions about the variation in RSL occurrence on steep slopes should be unaffected.

There is some difficulty in distinguishing RSL from topographic shading or slope streaks; also, observational biases like phase angle and illumination angle at the time of image acquisition can affect our results. To minimize the effect of observational bias, we only considered RSL confirmed when recurrence was observed at the same general location to rule out episodic dry flows. Examination of image sequences where phase angle varies strongly within a short time period show that this does not significantly affect our ability to detect the presence and distribution of RSL (McEwen et al., 2011). The dustiness of the air seems to be the largest observational variable, exacerbated by large spacecraft rolls that increase the path length. The viewing and illumination angle can also affect our ability to confidently identify RSL. Since HiRISE acquires images at ~3 PM local time, this may explain why we observe more RSL on west (Sun)-facing slopes than on east-facing slopes. The distribution of HiRISE images over Mars contains another bias: during southern summer, there is denser HiRISE coverage of the southern hemisphere than of equatorial or northern latitudes (Fig. 2). This is mostly due to active monitoring of mid-latitude gullies and RSL and favoring well-illuminated targets. The global distribution of RSL appears consistent with primary control by temperature and surface properties such as albedo and thermal inertia. They are absent from the very high elevations (>2 km; corresponding to atmospheric pressure of ~5 mbar (Smith and Zuber, 1998)) because these areas are bright and dust-covered, effectively insulating the sub-surface. They are either absent or rare in the northern hemisphere because northern summer solstice occurs near aphelion.

8.2. Seasonality and surface temperature

As noted above, RSL in the southern mid-latitudes form and grow almost exclusively during southern summer. However, inter-annual variability in number of RSL and their active season is observed at most sites. For example, in MY 28 and following the dust storms of 2007, incremental growth of RSL was observed as late as L_s 11–20° (well into the start of MY 29) at some sites (Table S4). In subsequent Mars years, the L_s range for RSL activity was much shorter where we did not observe RSL growth past L_s 321°, and L_s 342° for MY 29 and MY 30. In a year to year basis, the surface temperature of RSL slopes do not vary to a significant extent; however, the reduction in number of RSL in MY 29 and MY 30 along with their shorter time of activity implies that the 2007 dust storm had an effect on RSL formation and growth. The dust storm either helped increase the surface temperature or availability of water or some other factor leading to higher RSL activity in MY 28, or made RSL more visible.

Confirmed RSL are also found to be active between L_s 50–288 at the fresh crater near Coprates Chasma, and at other sites around Valles Marineris. The RSL at these locations have different seasonal behavior (McEwen et al., 2014). Although extremely rare, examples of RSL from southern mid-latitude that exhibit different seasonal behavior is also observed. For example, an image of Horowitz crater, ESP_027623_1475 at 32°S, shows that some activity occurred sometime between L_s 20–126.

The strong correlation of RSL activity with season implies a crucial role temperature plays in their formation. Brightness temperature we report in Table S2 were averaged over all slopes where RSL are present. Additionally, an isotropic emission, unit emissivity and zero atmospheric optical depth are assumed for these measurements so they represent minimum values for actual surface temperature. THEMIS mostly acquires images during late afternoon, so the temperature we derived is not the peak temperature for all slope orientations (Fig. 12). During the period when we observe RSL growth, THEMIS temperature (if available) lies in the range of 250–290 K. Our thermal model also suggests temperature higher than 273 K for all confirmed RSL sites (Fig. 12a and b). However, the peak temperatures at 10 cm depth never exceed 273 K.

8.3. Formation mechanism

The strong seasonal, latitudinal and slope-aspect trends suggest that RSL require relatively warm temperatures to form. The temperature range during their formation time is ideal for water-based solutions, but no OH^- or H_2O related spectral signatures have been detected on RSL slopes by the Compact Reconnaissance Imaging Spectrometer for Mars (CRISM; Murchie et al., 2007) (Ojha et al., 2013). The compositional characterization of RSL is especially challenging because most RSL are much smaller than the ~18 m/pixel scale of CRISM data, but even on the slopes hosting the widest RSL, spectral features diagnostic of water are not observed. Ojha et al. (2013) however noticed some spectral fluctuation on RSL slopes that are consistent with either removal of a fine-grained surface component during RSL flow, precipitation of ferric oxides, and/or wetting of the substrate.

Water would not persist on Mars' surface for long. The absorptions expected for a wet surface would vanish rapidly when exposed to desiccating conditions, even while the surface still retains its darkened albedo (Massé et al., 2012). Even aqueous solutions formed via deliquescence of perchlorate salts will only be stable for a few hours of the day on Mars' surface (Gough et al., 2011).

Stillman et al. (2013) argued that freshwater (minimal saltiness) could explain RSL activity because the surface temperatures probably exceed 273 K when they are actively growing, but the stability of pure water on Mars surface is even more unlikely. At the hottest times of day, temperatures decrease with depth, as supported by our thermal model (Fig. 12c and d), so if RSL have a subsurface origin then the freezing point (depending on the depth to sub-surface H_2O) may be depressed (Chevrier and Rivera-Valentin, 2012). RSL could be purely surface phenomena if they form via deliquescence of salts, but then the water is necessarily highly salty. Melting of seasonal frost can also cause RSL flow, but at the times and places when RSL form, frost should not persist on the surface. Carrozzo et al. (2009) found spectroscopic evidence for ice at tropical latitudes between 15°S and 30°S, but this was during L_s 99–150, when RSL are not observed to form. Pure water is also not stable over much of Mars' surface (Ingersoll, 1970), and temperature from THEMIS images and our model imply some RSL activity appears to occur below the freezing point of pure water (Table S2, Fig. 12).

Calcium chloride (Knauth and Burt, 2002), sodium chloride (Sears et al., 2002) and ferric sulfate (Chevrier and Altheide, 2008) have been proposed to form martian brines and are stable at low temperatures. The eutectic temperature of perchlorate solutions is 236 K for sodium perchlorate and 206 K for magnesium perchlorate, the lowest of any salt yet identified on Mars (Chevrier et al., 2009; Marion et al., 2010; Pestova et al., 2005). Besides forming brines at low temperatures, they also readily absorb water vapor from the atmosphere and deliquesce, providing a possible source of water for RSL formation. The phase transition from crystalline to aqueous state during deliquescence occurs when the relative humidity (RH) is equal to or greater than the deliquescence relative humidity (DRH) of the salt. Gough et al. (2011) predict that during the late morning and evening, either stable or metastable aqueous perchlorate solutions can exist at certain locations. However, it is not clear whether this mechanism can supply significant volumes of water since the relative humidity may be low during the day, and MRO acquires observations in the late afternoon so no aqueous bands may be detectable via CRISM.

Antarctic water tracks have been proposed as a terrestrial analog for RSL (Levy, 2012). By comparing the hydrological properties of the water track substrate with remote sensing observations of RSL, Levy (2012) supported the hypothesis of McEwen et al. (2011) that RSL form through the downslope flow of brines. Laboratory experiments conducted by Conway et al. (2011) have provided insights into the water flow formation mechanism. They were able to produce water flows under low temperatures (0.5–5 °C) and low pressures (7 mbar) comparable to those on the present-day martian surface (by introducing the water via a pipe). Conway et al. (2011) also reported that small but detectable channels and fans formed on one occasion when they used poorly sorted crushed igneous rocks as the substrate. They noticed that the depositional fan was entirely composed of the finer material, and coarser material was not transported, which is consistent with the morphology of fans we see at the toes of RSL (Figs. 1 and 3).

Although laboratory modeling and terrestrial analogs help shed light on their possible formation mechanism, there are still many unanswered questions about RSL, especially concerning their origin and potential sources of water. Compositional information would be key, and the search for associated spectral signatures is ongoing with CRISM. Laboratory experiments with briny flows in Mars environmental chambers (e.g., Addison et al., 2010) may prove diagnostic, if they can reproduce the detailed observations.

9. Conclusions

A survey of new HiRISE images from southern summer combined with data from previous studies has given us insights into the geological and morphological settings of RSL. Compared to previous studies, we have identified new RSL sites, confirmed old candidate sites and have been able to put better constraints on their seasonality. We have now confirmed RSL locations at 13 different sites in the southern hemisphere in addition to 8 partially confirmed RSL sites with recurrence verified. Surface properties, slope preference, seasonality and regional scale surface temperature for all the confirmed RSL and partially confirmed sites whose recurrence have been verified are reported here (Table S2).

From our observations of their latitudinal, slope orientation, steepness, surface morphology and seasonal preference, and our survey of all HiRISE images over the southern summer of MY 30 and 31, we conclude that RSL are a unique phenomenon on Mars, clearly distinct from other slope processes that occur near the poles or in dusty terrains (e.g., Chuang et al., 2007; Kereszturi et al., 2009). Although the formation mechanism for RSL is still uncertain, their morphology, geological setting and seasonality are consistent with wet flow. However, spectroscopic data have yet to detect H_2O or remnant salts formed by evaporation, and the source of water for RSL remains unclear. Further compositional and laboratory work is essential to understand the nature and formation mechanism of RSL.

Acknowledgments

We thank Joe Levy and an anonymous reviewer for comments that improved the manuscript. We are grateful to the Mars Reconnaissance Orbiter HiRISE team for financial, operational and scientific support.

Appendix A. Supplementary material

Supplementary data associated with this article can be found, in the online version, at http://dx.doi.org/10.1016/j.icarus.2013.12.021.

References

Addison, B.C., Chevrier, V.F., Dixon, J.C., Howe, K.L., 2010. Experimental simulations of martian gullies using $MgSO_4$ brine solution. Lunar Planet. Sci. 41, #1399.
Baker, V.R., 1982. The Channels of Mars. Univ. of Texas Press, Austin.
Brass, G.W., 1980. Stability of brines on Mars. Icarus 42 (1), 20–28.
Carr, M.H., 1995. The martian drainage system and the origin of valley networks and fretted channels. J. Geophys. Res. 100 (E4), 7479–7507.
Carrozzo, F.G., Bellucci, G., Altieri, F., D'Aversa, E., Bibring, J.P., 2009. Mapping of water frost and ice at low latitudes on Mars. Icarus 203 (2), 406–420.
Chevrier, V.F., Altheide, T.S., 2008. Low temperature aqueous ferric sulfate solutions on the surface of Mars. Geophys. Res. Lett. 35, L22101. http://dx.doi.org/10.1029/2008GL035489.
Chevrier, V.F., Rivera-Valentin, E.G., 2012. Formation of recurring slope lineae by liquid brines on present-day Mars. Geophys. Res. Lett. 39, L21202. http://dx.doi.org/10.1029/2012GL054119.
Chevrier, V.F., Hanley, J., Altheide, T.S., 2009. Stability of perchlorate hydrates and their liquid solutions at the Phoenix landing site, Mars. Geophys. Res. Lett. 36 (10), L10202.
Christensen, P.R. et al., 2001. Mars global surveyor thermal emission spectrometer experiment: Investigation description and surface science results. J. Geophys. Res. E: Planets 106 (E10), 23823–23871.
Christensen, P.R. et al., 2004. The Thermal Emission Imaging System (THEMIS) for the Mars 2001 Odyssey Mission. Space Sci. Rev. 110 (1/2), 85–130.
Chuang, F.C., Beyer, R.A., McEwen, A.S., Thomson, B.J., 2007. HiRISE observations of slope streaks on Mars. Space Sci. Rev. 110 (1/2), 85–130.
Clancy, R.T. et al., 2000. An intercomparison of ground-based millimeter, MGS TES, and Viking atmospheric temperature measurements: seasonal and interannual variability of temperatures and dust loading in the global Mars atmosphere. J. Geophys. Res. 34 (20), 9553–9571.
Conway, S.J., Balme, M.R., Murray, J.B., Lamb, M.P., Towner, M.C., 2011. Enhanced runout and erosion by overland flow at low pressure and sub-freezing conditions: Experiments and application to Mars. Icarus 105 (E4), 9553–9571.

Diniega, S., Byrne, S., Dundas, C.M., McEwen, A.S., Bridges, N.T., 2011. Seasonality of present-day martian dune-gully activity. Geology 211 (1), 443–457.

Dundas, C.M., Byrne, S., 2010. Modeling sublimation of ice exposed by new impacts in the martian mid-latitudes. Icarus 37 (7), L07202–L07728.

Dundas, C.M., Diniega, S., Hansen, C.J., Byrne, S., McEwen, A.S., 2012a. Seasonal activity and morphological changes in martian gullies. Icarus 38 (11), 1047–1050.

Dundas, C.M., McEwen, A.S., Diniega, S., Byrne, S., Martinez-Alonso, S., 2012b. New and recent gully activity on Mars as seen by HiRISE. Geophys. Res. Lett. 220 (1), 124–143.

Gorelick, N.S. et al., 2003. JMARS: A multimission data fusion application. Lunar Planet. Sci. XXXIV. Abstract 2057.

Gough, R.V., Baustian, K.J., Wise, M.E., Tolbert, M.A., Chevrier, V.F., 2011. Laboratory studies of perchlorate phase transitions: Support for metastable aqueous perchlorate solutions on Mars. Earth Planet. Sci. Lett. 312 (3–4), 371–377.

Hansen, C.J. et al., 2011. Seasonal erosion and restoration of Mars' northern polar dunes. Science 331 (6017), 575–578.

Hansen, C.J., Bourke, M., Byrne, S., McEwen, A., Portyankina, G., Pommerol, A., Thomas, N., Dundas, C., Mellon, M., 2012. Observations of the northern seasonal polar cap on Mars: I. Spring sublimation activity and processes. Icarus 225 (2), 881–897.

Hecht, M.H., 2002. Metastability of liquid water on Mars. Icarus 156 (2), 373–386.

Ingersoll, A.P., 1970. Mars: Occurrence of liquid water. Science 168, 972–973.

Kereszturi, A., Berczi, S., Ganti, T., Sik, A., Horvath, A., Möhlmann, D., Kuti, A., 2009. Recent rheologic processes on dark polar dunes of Mars: Driven by interfacial water? Icarus 201 (2), 492–503.

Knauth, L.P., Burt, D.M., 2002. Eutectic brines on Mars: Origin and possible relation to young seepage features. Icarus 158 (1), 267–271.

Kreslavsky, M.A., Head, J.W., 2003. North-south topographic slope asymmetry on Mars: Evidence for insolation-related erosion at high obliquity. Geophys. Res. Lett. 30 (15), PLA 1-1–1-4.

Levy, J., 2012. Hydrological characteristics of recurrent slope lineae on Mars: Evidence for liquid flow through regolith and comparisons with Antarctic terrestrial analogs. Icarus 219 (1), 1–4.

Malin, M.C., Edgett, K.S., 2000. Evidence for recent groundwater seepage and surface runoff on Mars. Science 288 (5475), 2330.

Marion, G.M., Catling, D.C., Claire, M.W., Zahnle, K.J., 2010. Modeling aqueous perchlorate chemistries with applications to Mars. Icarus 207 (2), 675–685.

McCauley, J.F., Carr, M.H., Cutts, J.A., Hartmann, W.K., Masursky, H., Milton, D.J., Sharp, R.P., Wilhelms, D.E., 1972. Preliminary mariner 9 report on the geology of Mars. Icarus 17 (2), 289–327.

McEwen, A.S. et al., 2007. Mars reconnaissance orbiter's high resolution imaging science experiment (HiRISE). J. Geophys. Res. E: Planets 112 (5). http://dx.doi.org/10.1029/2005JE002605.

McEwen, A.S. et al., 2010. The High Resolution Imaging Science Experiment (HiRISE) during MRO's Primary Science Phase (PSP). Icarus 205 (1), 2–37.

McEwen, A.S. et al., 2011. Seasonal flows on warm martian slopes. Science 333 (6043), 740–743.

McEwen, A.S., Dundas, C.M., Mattson, S.S., Toigo, A.D., Ojha, L., Wray, J.J., et al., 2014. Recurring slope lineae in equatorial regions of Mars. Nat. Geosci. 7 (1), 53–58.

Mellon, M.T., Jakosky, B.M., Kieffer, H.H., Christensen, P.R., 2000. High-resolution thermal inertia mapping from the Mars global surveyor thermal emission spectrometer. Icarus 148 (2), 437–455.

Murchie, S. et al., 2007. Compact reconnaissance imaging spectrometer for Mars (CRISM) on Mars reconnaissance orbiter (MRO). J. Geophys. Res. E: Planets 112 (E5), 1–57.

Ojha, L.L., Wray, J.J., Murchie, S.L., Mcewen, A.S., Wolff, M.J., Karunatillake, S.S., 2013. Spectral constraints on the formation mechanism of recurring slope lineae. Geophys. Res. Lett. 40. http://dx.doi.org/10.1002/2013GL057893.

Pestova, O.N., Myund, L.A., Khripun, M.K., Prigaro, A.V., 2005. Polythermal study of the systems $M(ClO_4)_2$–H_2O ($M^{2+} = Mg^{2+}, Ca^{2+}, Sr^{2+}, Ba^{2+}$). Russ. J. Appl. Chem. 78 (3), 409–413. http://dx.doi.org/10.1007/s11167-005-0306-z.

Pouliquen, O., 1999. Scaling laws in granular flows down rough inclined slopes. Phys. Fluids 11 (2–3), 542–548.

Presley, M.A., Christensen, P.R., 1997. The effect of bulk density and particle size sorting on the thermal conductivity of particulate materials under martian atmospheric pressures. J. Geophys. Res. E: Planets 102 (E4), 9221–9229.

Putzig, N.E., Mellon, M.T., Kretke, K.A., Arvidson, R.E., 2005. Global thermal inertia and surface properties of Mars from the MGS mapping mission. Icarus 173 (2), 325–341.

Putzig, N.E., Mellon, M.T., 2007. Apparent thermal inertia and the surface heterogeneity of Mars. Icarus 191, 68–94. http://dx.doi.org/10.1016/j.icarus.2007.05.013.

Ruff, S.W., Christensen, P.R., 2002. Bright and dark regions on Mars: Particle size and mineralogical characteristics based on thermal emission spectrometer data. J. Geophys. Res. E: Planets 107 (12), 10–11.

Sears, D.W.G. et al., 2002. Investigation of biological, chemical and physical processes on and in planetary surfaces by laboratory simulation. Planet. Space Sci. 50 (9), 821–828.

Smith, D.E., Zuber, M.T., 1998. The relationship between MOLA northern hemisphere topography and the 6.1-Mbar atmospheric pressure surface of Mars. Geophys. Res. Lett. 25 (24), 4397–4400.

Stillman, D.E., Grimm, R.E., Michaels, T.I., Harrison, P., 2013. Formation of Recurrent Slope Lineae (RSL) by freshwater discharge of melted cold traps. Lunar Planet. Sci. 44, #1737.

Zent, A.P., Fanale, F.P., Roth, L.E., 1990. Possible martian brines: radar observations and models. J. Geophys. Res. 95 (B9), 14531–14542.

Zurek, R.W., Smrekar, S.E., 2007. An overview of the Mars reconnaissance orbiter (MRO) science mission. J. Geophys. Res. Part E: Planets 112 (E5), 1–22.